Molecular Biology of the Cell
Vol. 15, 5369–5382, December 2004

The Endo-Lysosomal Sorting Machinery Interacts with the Intermediate Filament Cytoskeleton[D]

Melanie L. Styers,*† Gloria Salazar,† Rachal Love,† Andrew A. Peden,‡ Andrew P. Kowalczyk,†§ and Victor Faundez†‖¶

*Graduate Division of Biological and Biomedical Sciences, Departments of †Cell Biology and §Dermatology, ‖Center for Neurodegenerative Diseases, Emory University, Atlanta, GA 30322; and ‡Genentech, Inc., South San Francisco, CA 94080-4990

Submitted March 31, 2004; Revised September 20, 2004; Accepted September 21, 2004
Monitoring Editor: Keith Mostov

Cytoskeletal networks control organelle subcellular distribution and function. Herein, we describe a previously unsuspected association between intermediate filament proteins and the adaptor complex AP-3. AP-3 and intermediate filament proteins cosedimented and coimmunoprecipitated as a complex free of microtubule and actin binding proteins. Genetic perturbation of the intermediate filament cytoskeleton triggered changes in the subcellular distribution of the adaptor AP-3 and late endocytic/lysosome compartments. Concomitant with these architectural changes, and similarly to AP-3-null *mocha* cells, fibroblasts lacking vimentin were compromised in their vesicular zinc uptake, their organellar pH, and their total and surface content of AP-3 cargoes. However, the total content and surface levels, as well as the distribution of the transferrin receptor, a membrane protein whose sorting is AP-3 independent, remained unaltered in both AP-3- and vimentin-null cells. Based on the phenotypic convergence between AP-3 and vimentin deficiencies, we predicted and documented a reduced autophagosome content in *mocha* cells, a phenotype previously reported in cells with disrupted intermediate filament cytoskeletons. Our results reveal a novel role of the intermediate filament cytoskeleton in organelle/adaptor positioning and in regulation of the adaptor complex AP-3.

INTRODUCTION

Adaptor complexes play a central role in membrane protein traffic by regulating the packing of membrane proteins into distinct vesicle carriers (Bonifacino and Traub, 2003; Robinson, 2004). Four distinct heterotetrameric adaptor complexes (AP-1 to AP-4) carry out compartment-selective sorting and vesiculation (Bonifacino and Traub, 2003; Robinson, 2004). Among these complexes, AP-3 is unique in that its function is highlighted by several vertebrate genetic deficiencies. In humans, defects in the AP-3 β3 subunit lead to Hermansky-Pudlak type II syndrome (Dell'Angelica *et al*., 1999; Huizing *et al*., 2002). A similar phenotype is observed in the alleles *pearl* and *mocha*, mice mutants that lack functional AP-3 β3 and δ subunits, respectively (Kantheti *et al*., 1998; Feng *et al*., 1999; Kantheti *et al*., 2003). From these genetic models, we have learned that AP-3 complexes regulate the sorting of a subset of lysosome, melanosome, hematopoietic granule, and synaptic vesicle-specific proteins (Faundez *et al*., 1998; Kantheti *et al*., 1998, 2003; Dell'Angelica *et al*., 1999; Salazar *et al*., 2004b). AP-3 regulates the composition of these organelles by controlling the exit of organelle-specific membrane proteins from endosomes en route to their final destinations (Peden *et al*., 2004; Salazar *et al*., 2004b).

In addition to adaptors, microtubule and actin-based cytoskeletal networks control the composition of membranous organelles (Gottlieb *et al*., 1993; Gaidarov *et al*., 1999; Nakagawa *et al*., 2000; Apodaca, 2001). Drugs affecting microtubule and actin polymerization have been instrumental in the identification of membrane protein trafficking and sorting processes that depend upon the functional integrity of these cytoskeletal networks (Gaidarov *et al*., 1999; Apodaca, 2001; Qualmann and Kessels, 2002). In contrast, a role for intermediate filaments in controlling adaptor-dependent membrane protein traffic remains largely unexplored, primarily due to a nonexistent intermediate filament pharmacology. Although intermediate filament function as a mechanical scaffold is well documented (Coulombe *et al*., 2000), multiple lines of evidence point to a role for these filaments in controlling the architecture and/or traffic through membranous organelles. For example, the formation of autophagocytic vacuoles, an organelle that converges with late endosomal compartments, depends upon the functional integrity of intermediate filament networks (Blankson *et al*., 1995; Kim and Klionsky, 2000). In addition, postendocytic low-density lipoprotein-cholesterol metabolism (Sarria *et al*., 1992; Holwell *et al*., 1999) and endosome-Golgi recycling of glycosphingolipids are decreased in cells lacking intermediate filaments (Gillard *et al*., 1994, 1998). Vimentin filaments are also known to bind to the Golgi complex through a Golgi-specific protein, although it is unknown whether this association controls transport functions to or through the Golgi (Gao and Sztul, 2001). Intermediate filaments also seem to control some membrane protein sorting events. In polarized epithelial cells, a subapical intermediate filament cytoskeleton regulates the apical-basolateral distribution of several

Article published online ahead of print. Mol. Biol. Cell 10.1091/mbc.E04–03–0272. Article and publication date are available at www.molbiolcell.org/cgi/doi/10.1091/mbc.E04–03–0272.

[D] The online version of this article contains supplemental material at MBC Online (http://www.molbiolcell.org).

¶ Corresponding author. E-mail address: faundez@cellbio.emory.edu.

membrane proteins (Salas *et al*., 1997; Ameen *et al*., 2001; Toivola *et al*., 2004) by mechanisms still not understood.

Here, we present a novel association between the intermediate filament cytoskeleton and the adaptor AP-3 through the AP-3 β3 subunit. The interaction between intermediate filaments and AP-3 could regulate the position of organelles and/or their membrane protein content. We tested these hypotheses by analyzing the subcellular distribution of AP-3 and different endosomal markers in intermediate filament-deficient cells. AP-3 and late endosomal/lysosomal reporter molecules were specifically redistributed in intermediate-deficient cells. In addition, AP-3–dependent phenotypes and changes in the content of AP-3–specific membrane protein cargoes were observed in fibroblasts lacking intermediate filaments. In summary, our results indicate that interactions between intermediate filaments and the adaptor complex AP-3 likely control the positioning, content, and subcellular distribution of selected late endosome/lysosome membrane proteins.

MATERIALS AND METHODS

Cell Culture and Transfection

SW13, MTF6, and MTF16 cells were a gift of Dr. Robert Evans (University of Colorado, Denver, CO) (Sarria *et al*., 1992; Holwell *et al*., 1997). These cell lines were cultured as described previously (Sarria *et al*., 1992; Holwell *et al*., 1997). Immortalized *mocha* fibroblasts transduced with an empty retrovirus or a retrovirus carrying the AP-3 delta subunit (Peden *et al*., 2004) were grown in DMEM medium (Cellgro, Herndon, VA) (4.5 g/l glucose) supplemented with 10% fetal calf serum (Hyclone Laboratories, Logan, UT), 100 U/ml penicillin, and 100 μg/ml streptomycin and hygromycin (200 μg/ml).

Antibodies

Monoclonals used were anti-peripherin and anti-actin C4 (Chemicon International, Temecula, CA), anti-tubulin DM1A, anti-MAP-2 (AP-20), anti-vimentin V9, anti-vinculin Vin11–5 (Sigma-Aldrich, St. Louis, MO), anti γ adaptin, anti-GM130, and anti-TGN38 (BD Biosciences, Franklin Lakes, NJ), anti-transferrin receptor (H68.4; Zymed Laboratories, South San Francisco, CA), anti-cathepsin D (Upstate Biotechnology, Charlottesville, VA), anti-KDEL receptor (StressGen, San Diego, CA), anti-HA (12CA5; a gift from Dr. Y. Altschuler, Tel Aviv University, Tel Aviv, Israel), anti-SV2 (10H4), anti-CD63 (H5C6), anti-LAMP I H4A3, anti-mouse Lamp I ID4B, Lamp II ABL-93, and anti δ (SA4) (Developmental Studies Hybridoma Bank, University of Iowa, Iowa City, IA). All AP-3 polyclonal antibodies have been described previously (Salem *et al*., 1998; Faundez and Kelly, 2000). Other polyclonal antibodies used were anti-peripherin and anti-glutathione *S*-transferase (GST) (Chemicon International), anti-cofilin (Cytoskeleton, Denver, CO), and anti-hamster vimentin #314 (a gift from Dr. Robert Goldman, Northwestern University, Chicago, IL). Anti-cation–independent mannose-6-phosphate receptor antibodies were a gift from Dr. Stuart Kornfeld (Washington University, St. Louis, MO).

Immunoprecipitations, Gradients, and Extractions

Brain cytosol was prepared as described (Clift-O'Grady *et al*., 1998). SW13 cell lysates were prepared in buffer A (10 mM HEPES, pH 7.4, 150 mM NaCl, 1 mM EGTA, and 0.1 mM $MgCl_2$) containing 0.1% Triton X-100. Soluble fractions were isolated by centrifugation at 16,100 $\times$ *g* for 30 min. Cells were then washed in Dulbecco's phosphate-buffered saline (DPBS), and Triton-soluble extracts were prepared as described above. Immunoprecipitations were performed as described previously (Faundez and Kelly, 2000). Brain cytosol was resolved on 5–20% sucrose gradients (Dell'Angelica *et al*., 1997).

Extractions were performed as described by Helfand *et al*. (2002) in the presence of 1% Triton X-100 on samples containing 500,000 cells. Band intensities were measured using the NIH Image 1.61 software (Faundez and Kelly, 2000). All data are presented as average $\pm$ SE. Statistical analysis was performed using a two-tailed *t* test.

In Vitro Binding Assays

cDNAs encoding vimentin, peripherin, and internexin, a gift from Dr. R. Liem (Columbia University Medical Center, NY), were subcloned into the vector pcDNA3.1. In vitro transcription/translation was performed using the TnT Rabbit Reticulocyte Lysate system according to manufacturer's protocol (Promega, Madison WI). Immunoprecipitated AP-3 complexes from rat brain cytosol were incubated with 25 μl of the transcription-translation reaction in buffer A containing 0.1% Triton X-100. In competition experiments, recombinant vimentin (Cytoskeleton) was added to a final concentration of 0.004 mg/ml in buffer A containing 0.1% Triton-X-100. Binding and washes were performed at 4°C in the presence of Complete antiprotease mixture. Washing beads three times for 10 min terminated incubations. Bound proteins were resolved by SDS-PAGE, and ^{35}S-labeled proteins were visualized by PhosphorImager.

Vimentin Overlay Assay

Immuno-isolated AP-3 complexes or purified GST-β3 fusions (Dell'Angelica *et al*., 1998) were resolved on 4–20% acrylamide gradient gels and transferred to nitrocellulose. After blocking, blots were incubated in 5 mM PIPES, pH 7.4, 0.5 mM dithiothreitol, 5% sucrose, 1% glycerol containing or not 500 ng/ml recombinant hamster vimentin (Cytoskeleton). After washing, blots were probed with anti-vimentin monoclonal antibodies (V9) to detect bound vimentin. GST fusion proteins were prepared as described previously (Faundez and Kelly, 2000).

Confocal Microscopy

Cells were fixed and processed for immunofluorescence as described previously (Faundez *et al*., 1997). Secondary antibodies used were Alexa-conjugated goat anti-mouse 488, goat anti-mouse 568, goat anti-rabbit 568 (Molecular Probes), and/or fluorescein isothiocyanate-conjugated goat anti-rat (Jackson ImmunoResearch Laboratories, West Grove, PA).

For internalization assays, SW13 cells were incubated with anti-CD63 antibodies in DMEM/F12 for 1 h at 4°C. After washing, cells were incubated at 37°C. Cells were then fixed and processed as described above. Transferrin internalization assays were performed with Alexa 568-conjugated human transferrin (Molecular Probes) as described previously (Faundez *et al*., 1997).

In vivo Lysosensor Green DND-189 staining and imaging was performed as described previously (Salazar *et al*., 2004b).

Both fixed and live specimens were viewed using an Axiovert 100M microscope (Carl Zeiss, Thornwood, NY) coupled to HeNe1 and argon ion lasers. Images were acquired using LSM 510 sp1 software (Carl Zeiss). The emission filters used for immunofluorescence and live imaging were BP 565-615 and BP 500-550 IR. All images were viewed and acquired using either a Plan Apochromat 63$\times$/1.4 oil DiC objective or a Plan Apochromat 100$\times$/1.4 oil DiC objective. All scale bars are 10 μm.

Monodansylcadaverine (MDC) Staining and Two-Photon Microscopy

Live MTF6, MTF16, *mocha*, or rescued *mocha* fibroblasts were seeded on 10-mm #0 MatTek dishes coated with Matrigel (BD Biosciences). After washing, cells were incubated in 50 μM MDC in DMEM/F12 for 10 min at 37°C. Cells were washed and imaged at room temperature in 10 mM glucose-DPBS with Ca^{2+}/Mg^{2+}. Specimens were viewed using an Axiovert 100M microscope (Carl Zeiss) coupled to a Coherent 5 W Verdi argon ion pumped Ti:Sapphire laser tuned at 750 nm. Images were acquired using LSM 510 Meta software. Using the channel mode, emission was taken using the BP 435-485 IR filter. All images were viewed and acquired using a Plan-Apochromat 63$\times$/1.4 oil DiC objective. Images were processed and analyzed using MetaMorph software, version 3.0 (Universal Imaging, Downingtown, PA). A color threshold was set to pixel intensities between 150 and 255, and regions were automatically selected and region area calculated by the software. All region areas greater than 10 were averaged for each image. The average areas per image within the same data set were averaged. Wild-type averages were then normalized to 100% for each data set. Analysis includes 10–14 images per data experiment. All experiments were performed between five and eight independent times.

Flow Cytometry

Cells were fixed and stained as described above. Surface staining was determined by staining cells in the absence of detergent. Total levels were assessed by staining in the presence of 0.02% saponin. Antibodies and Lysosensor fluorescence were analyzed using a FACscalibur System (BD Biosciences). Results were analyzed using FloJo version 4.4.4 (Treestar, Ashland, OR). Averages are of three to six samples, each containing 10,000 cells. To depict the data in a normalized manner, we use percentage of maximum.

Zinc and Lysosensor Green DND-189 uptake was performed as described previously (Salazar *et al*., 2004b). After zinquin, Lysosensor, or MDC staining, cells were washed at 4°C. Except for Lysosensor, fluorescence was determined using a MoFlo High Performance Cell Sorter from DakoCytomation (Fort Collins, CO). Zinquin and MDC were excited at 305 nm. The filters used were a 440 long pass and a 450/65 in front of the photo multiplier tube. Data analysis was performed as described above.

Biotinylation

Biotinylation was performed as described previously (Salazar and Gonzalez, 2002).

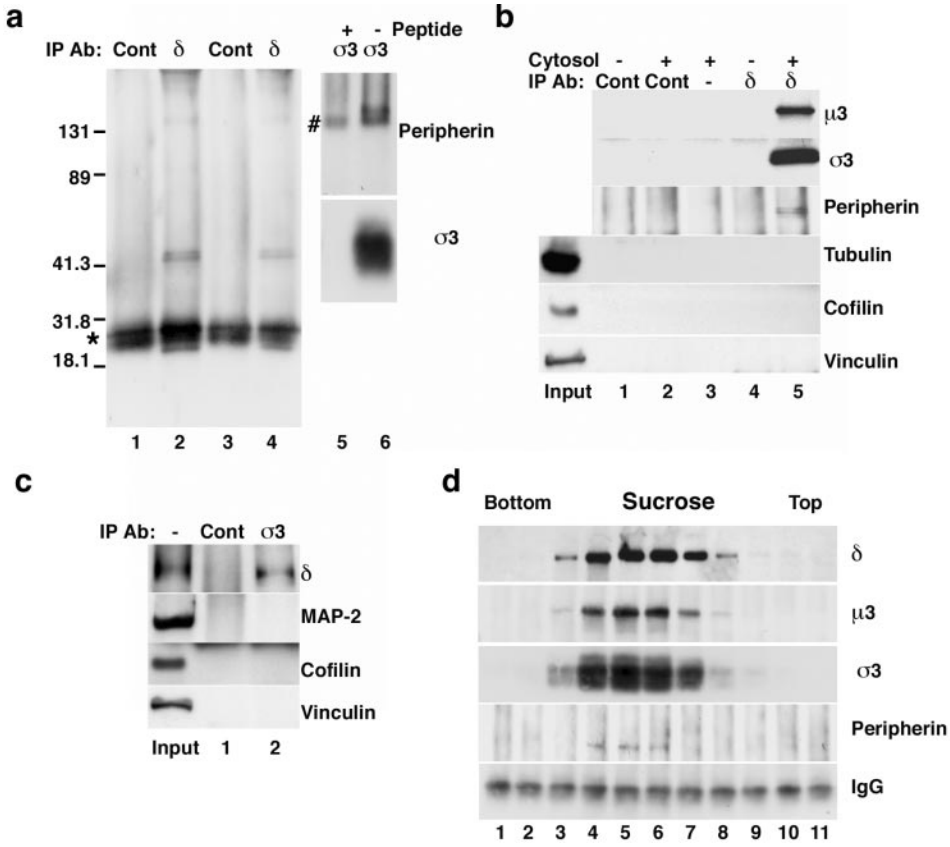

Figure 1. The adaptor complex AP-3 interacts with the intermediate filament peripherin. (a) Adult brain cytosol (lanes 1 and 2) and Triton-soluble extracts from newborn brain (lanes 3 and 4) or adult spinal cord (lanes 5 and 6) were immunoprecipitated with delta (δ) mAb (lanes 2 and 4) or sigma 3 (σ3) polyclonal antibody (lanes 5 and 6). Control immunoprecipitations were performed using the 10H4 mAb (lanes 1 and 3) or competing with antigenic peptides (lane 5). Peripherin was specifically associated with AP-3 immunocomplexes as detected with a polyclonal peripherin antibody (lanes 1–6). The asterisk on the left marks the light chain of the mouse IgG, whereas # marks the heavy chain of the rabbit anti-σ3 IgG. (b) Beads without antibodies (lane 3) or coated with the 10H4 control (lanes 1 and 2) or δ (lanes 4 and 5) monoclonal antibodies were incubated in the absence lanes 1 and 4) or presence (lanes 2, 3, and 5) of brain cytosol. Immunocomplexes were probed for AP-3 (μ3 and σ3), peripherin, tubulin, cofilin, and vinculin. No microtubules or actin-associated proteins were detected in the AP-3–peripherin complexes. (c) Beads coated with preimmune antibodies (lane 1) or σ3 (lane 2) polyclonal antibodies were incubated in the presence of brain cytosol. Immunocomplexes were MAP-2 and actin-binding protein free. (d) Adult brain cytosol was fractionated by sucrose sedimentation, and individual fractions were immunoprecipitated with delta subunit monoclonal antibodies and blotted with polyclonal antibodies against AP-3 subunits (δ, μ3, and σ3) and peripherin. AP-3 and peripherin cosediment as a complex. Bottom, mouse IgG light chains. Inputs in b and c are 10% of the total.

RESULTS

Intermediate Filament Proteins Interact with the Adaptor Complex AP-3

To isolate novel AP-3–interacting proteins, we performed affinity chromatography of native rat brain cytosol by using a monoclonal antibody (mAb) against the ear domain of the AP-3 δ subunit (Peden *et al*., 2004). Isolated immuno-complexes resolved by two-dimensional gel electrophoresis revealed a band of ~50 kDa and a pI value of 5, distinct from the μ3 AP-3 subunits (our unpublished data). Mass spectrometry identified six nonoverlapping peptides belonging to the intermediate filament peripherin (NM_012633; theoretical mol. wt. of 53.5; pI value of 5.2). Due to their abundance and physicochemical properties, cytoskeletal proteins may nonspecifically interact with the adaptor complex. Thus, we took several approaches to exclude this possibility. First, we performed our immunoprecipitations out of soluble extracts in which AP-3 is abundant, yet proteins that remain preponderantly insoluble, such as intermediate filaments, are poorly represented. We tested the putative AP-3–peripherin interaction by immunoprecipitation from native cytosol and Triton X-100–soluble brain extracts. In these extracts, peripherin levels were under the detection limit, yet tubulin, actin, and their binding proteins were abundant. We reasoned that immunoprecipitates containing AP-3 and peripherin but devoid of microtubule and actin cytoskeletal proteins would provide an indication of selectivity. AP-3 was immunoprecipitated with monoclonal antibodies against δ (Figure 1a, lanes 2 and 4) or affinity-purified anti-σ3 peptide antibodies (Figure 1a, lanes 5 and 6) followed by immunoblot with polyclonal or monoclonal (our unpublished data) antibodies against peripherin (Figure 1a, lanes 1–6). Peripherin was specifically immunoprecipitated by both AP-3 antibodies either from adult brain cytosol (Figure 1a, compare lanes 1 and 2), newborn brain (Figure 1a, compare lanes 3 and 4), or spinal cord detergent-soluble extracts (Figure 1a, compare lanes 5 and 6), yet controls with irrelevant antibodies (Figure 1a, lanes 1 and 3) or competition with the antigenic σ3 peptide (Figure 1a, lane 5) did not precipitate peripherin. Under these conditions, the binding of other cytoskeletal proteins to AP-3 was negligible. AP-3 immunoprecipitates were free of tubulin (Figure 1b) and other microtubule-associated proteins such as MAP-2 (Figure 1c), tau, and the coiled-coil containing kinesin heavy chain (our unpublished data). In addition, the actin binding proteins cofilin, vinculin (Figure 1, b and c), and α-actinin (our unpublished data) did not bind AP-3. Moreover, in immunoprecipitations using both control and specific antibodies, we detected low nonspecific binding of actin to beads (our unpublished data). These are stringent controls because these cytoskeletal proteins are particularly abundant in our extracts; moreover, α- and β-tubulin isoelectric points and molecular weight are almost identical to those of peripherin (http://ca.expasy.org/sprot/). Therefore, a simple electrostatic AP-3–peripherin interaction is unlikely. These results exclude nonspecific binding of AP-3 to a phys-

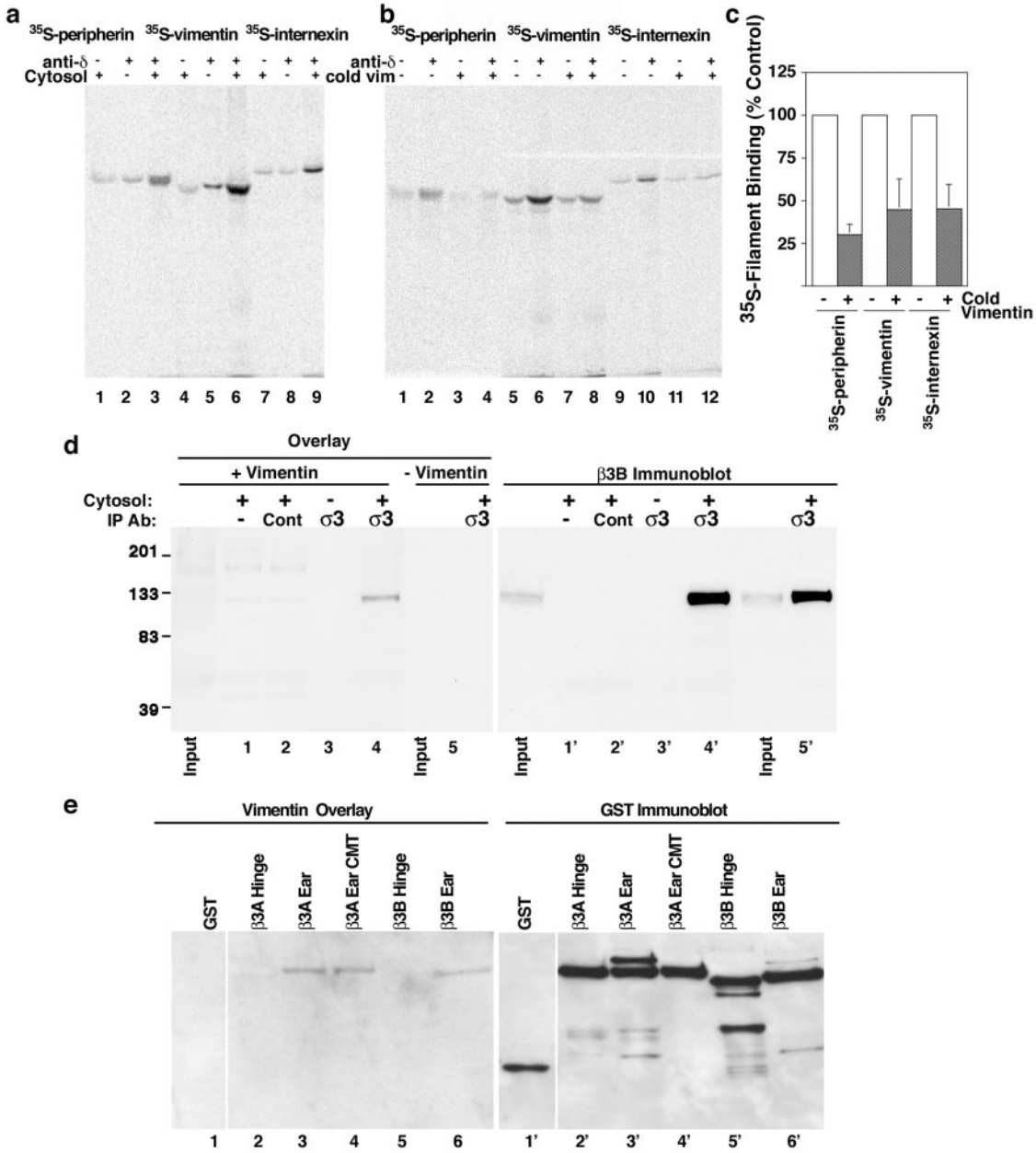

Figure 2. Various intermediate filaments bind AP-3 competitively. (a) Beads coated without (lanes 1, 4, and 7) or with δ mAb (lanes 2, 3, 5, 6, 8, and 9) were incubated in the absence (lanes 2, 5, and 8) or presence (lanes 1, 3, 4, 6, 7, and 9) of brain cytosol as a source of AP-3. Complexes were washed and challenged with in vitro transcribed-translated peripherin (lanes 1–3), vimentin (lanes (4–6), or internexin (lanes 7–9). Intermediate filaments specifically bind only when AP-3 is present (compare lanes 1–3, 4–6, and 7–9). (b) Bead-bound complexes were challenged with in vitro transcribed-translated vimentin, peripherin, or internexin in the absence (lanes 2, 6, and 10) and presence of recombinant cold vimentin (lanes 4, 8, and 12). After binding of the ^{35}S-labeled filaments, beads were washed and bound filament proteins were detected by PhosphorImager. Labeled filaments bound specifically to beads where AP-3 was present. Binding was displaced by cold recombinant vimentin. Controls included beads incubated with cytosol, but lacking antibody (lanes 1, 3, 5, 7, 9, and 11). (c) Graph depicts the quantification of ^{35}S-labeled filaments competition with cold recombinant vimentin (n = 3, triplicate determinations each). (d) Beads coated with no antibody (lane 1), control preimmune antibodies (lane 2), or σ3 antibodies (lanes 3–5) were incubated in the absence (lane 3) or presence (lanes 1, 2, 4, and 5) of brain cytosol as a source of AP-3. Immunoprecipitated proteins were resolved by SDS-PAGE and transferred to membranes that were incubated with (lanes 1–4) or without (lane 5) recombinant vimentin. A band of 120-kDa specifically binds vimentin. This band comigrates with the β3 AP-3 subunit. Lanes 1′-5′ corresponds to lanes 1–5 after stripping and probing with a β3 mAb (depicted is one experiment representative of four). Inputs correspond to 10% of the cytosol used for immunoprecipitation. (e) One microgram of purified GST (lane 1) or fusion proteins encompassing the hinge domains of β3A and β3B (lanes 2 and 5), the ear domains of β3A (lanes 3 and 4) and β3B (lane 6), were resolved by SDS-PAGE, transferred to nitrocellulose, and incubated in presence of recombinant vimentin. Bound filament protein was revealed as described in text. Vimentin bound only the ear domains of the β3A and β3B subunits. Alanine substitution of the clathrin-binding site in β3A ear domain does not affect vimentin binding (compare lanes 3 and 4). No signal was detected in the absence of vimentin (our unpublished data). Lanes 1′-6′ represent the same gel probed with anti-GST antibodies. Data are a representative example of six independent experiments.

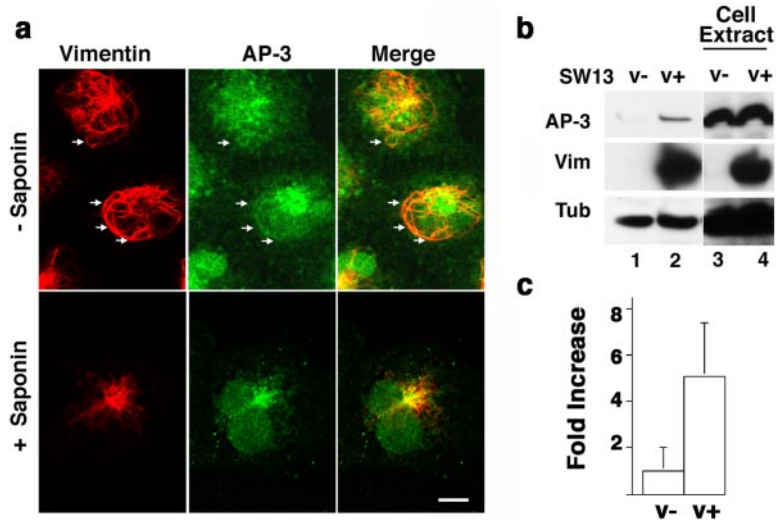

Figure 3. AP-3 associates with intermediate filament networks in SW13 V(+) cells. (a) SW13 vimentin-positive (v+) cells were perforated or not with saponin before fixation. AP-3 complexes were detected by immunofluorescence with δ monoclonal antibodies and vimentin with a polyclonal antibody. Arrows denote filaments decorated with AP-3 immunoreactivity. Experiments were done at least in duplicate coverslips (n = 3), and five to 10 random fields were imaged per coverslip. (b) SW13 vimentin positive (v+) and negative (v−) cells were extracted with 1% Triton X-100 at 4°C. Detergent-insoluble extracts (lanes 1 and 2) and input (lanes 3 and 4) were analyzed by immunoblot with AP-3 antibodies (δ and σ3, the latter not shown), vimentin, and tubulin antibodies. AP-3 remains associated with insoluble extracts in a vimentin-dependent manner. (c) Quantification of the results presented in b. Data were normalized to the amount of adaptor present in the detergent insoluble pool of SW13 v− cells (n = 3).

icochemically diverse set of abundant cytoskeletal proteins. In summary, our data fulfill these criteria for specificity of an AP-3–peripherin interaction.

We further tested the hypothesis that AP-3 and peripherin interacted as a complex by size fractionation of adult brain cytosol in sucrose gradients, followed by immunoprecipitation of the fractions with AP-3 antibodies (Figure 1d). Peripherin was immunoprecipitated only in those fractions in which AP-3 was present (Figure 1d, lanes 4–6). We used the kinesin heavy-light chain complex as a control. Although this complex overlapped with AP-3 in sucrose sedimentation, no kinesin heavy chains were immunoprecipitated by AP-3 antibodies (our unpublished data).

Peripherin forms part of the intermediate filament cytoskeleton in neurons (Djabali *et al*., 1993; Landon *et al*., 2000), yet AP-3 expression and function are widespread, thus suggesting that other tissue-specific intermediate filament proteins also could bind AP-3. We tested this hypothesis by analyzing in vitro the interaction of structurally and functionally related filament proteins representative of mesoderm- (vimentin) and neuroectoderm-derived tissues (peripherin and internexin). We first determined the binding specificity of radiolabeled filament proteins to δ antibody-immobilized AP-3. Radiolabeled peripherin, vimentin, or internexin were incubated with beads alone (Figure 2a, lanes 1, 4, and 7), bead–antibody complexes (Figure 2a, lanes 2, 5, and 8), or bead–antibody–AP-3 complexes (Figure 2a, lanes 3, 6, and 9). Bound ^{35}S-labeled filament proteins were resolved by SDS-PAGE and visualized by PhosphorImager. Binding of these proteins to immunoisolated AP-3 was ~8- to 10-fold higher than their binding to beads or the δ antibody itself. Using this assay, we analyzed whether the binding of different filament proteins was competitive. Immunoisolated AP-3 was incubated with in vitro ^{35}S-labeled intermediate filament proteins in the absence or presence of competing recombinant cold vimentin (Figure 2b, compare lanes 2 and 4, 6 and 8, 10 and 12). Unlabeled recombinant vimentin, added at a concentration significantly below the critical concentration for polymerization, efficiently competed with each of the ^{35}S-labeled filament proteins. In contrast, the nonspecific binding of ^{35}S-labeled vimentin to beads alone was minimally displaced by cold vimentin (Figure 2b compare lanes 1 and 3, 5 and 7, and 9 and 11). These results suggest that intermediate filament proteins competitively bind to the AP-3 complex.

To further document the AP-3–intermediate filament protein interaction, we sought to determine which subunit of the AP-3 heterotetramer binds intermediate filament proteins. We explored this question using vimentin overlay assays (Figure 2d), a technique successfully used to analyze the biochemical nature of vimentin interactions observed in vivo (Gao and Sztul, 2001). We took advantage of the fact that the AP-3 subunits can be readily identified by their characteristic SDS-PAGE migration as four distinct subunits. AP-3 was immunoprecipitated from brain cytosol by using polyclonal antibodies against the σ3 subunit of AP-3 (Figure 2d, lanes 4 and 5). Controls were performed with beads alone (Figure 2d, lane 1), preimmune IgG (Figure 2d, lane 2), or beads coated with σ3 antibodies yet lacking AP-3 (Figure 2d, lane 3). AP-3 subunits were resolved by SDS-PAGE and transferred to membranes, which were subsequently incubated in the presence (lanes 1–4) or absence (Figure 2d, lane 5) of recombinant vimentin. The intermediate filament protein present on the membrane was detected by immunoblot with a monoclonal vimentin antibody. Vimentin bound specifically to a band of ~120 kDa, a molecular mass consistent with the β3 subunit. This band was predominantly detected in those lanes containing AP-3 (Figure 2d, compare lanes 4 with 1–3, and 4′ with 1′–3′). Moreover, its detection was strictly dependent upon the inclusion of vimentin on the overlay step (Figure 2d, lane 5). The 120-kDa band perfectly coaligned with β3 (Figure 2d, compare lanes 4 and 4′), suggesting that β3 could interact with vimentin. We confirmed that β3 indeed binds vimentin in overlay assays by using GST-fusion proteins encompassing different domains of the ubiquitous (β3A) and neuronal-specific isoforms (β3B) of β3 (Figure 2e). Vimentin strongly interacted with the β3A and β3B ear domains (Figure 2e, lanes 3 and 6) as well as a β3A ear domain containing an alanine substitution of the clathrin binding site (Figure 2e, lane 4) (Dell'Angelica *et al*., 1998). However, vimentin binding to GST (Figure 2e, lane 1) and the hinge domains of β3A and B (Figure 2e, lanes 2 and 5) was negligible. Thus, these results demonstrate that intermediate filament proteins directly bind to a discrete domain in the β3 subunit of the adaptor complex.

In summary, our biochemical analysis indicates that AP-3 and peripherin selectively interact in a protein complex free of microtubule and actin cytoskeletal proteins. Furthermore, AP-3 interactions are not restricted to peripherin, because other closely related intermediate filament proteins, vimen-

tin and internexin, bind AP-3 in a competitive manner. In addition, this interaction is likely to occur via the ear domain of the β3 subunit.

The Vimentin Intermediate Filament Network Interacts with the Adaptor Complex AP-3

The interaction of AP-3 with the vimentin intermediate filament network was explored in SW13v+ carcinoma cells. This cell line expresses vimentin as the only intermediate filament protein. In addition, it offers the advantage of the clonal variant, SW13v−, which lacks intermediate filaments, although it possesses normal microtubule and actin cytoskeletons (our unpublished data) (Hedberg and Chen, 1986). First, we analyzed the interaction between AP-3 and vimentin by immunofluorescence microscopy of intact SW13v+ cells and cells extracted with detergent before fixation (Figure 3a). AP-3–containing organelles were detected in close apposition to vimentin filaments in intact cells. After detergent extraction, organelle-associated AP-3 was removed, yet the filamentous AP-3, detected either with antibodies to δ or σ3 subunits, remained bound (Figure 3a; our unpublished data). We further analyzed whether AP-3 could associate with detergent-insoluble cytoskeletons of SW13 v+ and v− cells (Figures 3, b and c). AP-3 remained bound to detergent-insoluble cytoskeletal networks from both cell lines, yet AP-3 binding was 5 times higher in extracts from SW13 cells expressing vimentin than in SW13v− cells (Figure 3b, compare 1 and 2; c). Adaptor content (Figure 3b, lanes 4 and 5) was identical in both cell lines. These results demonstrate that AP-3 decorates and interacts with intermediate filament networks in cultured cells.

The Intermediate Filament Cytoskeleton Controls the Positioning of the AP-3 Adaptor and Late Endosomal-Lysosomal Compartments

By virtue of their binding to AP-3, intermediate filaments could play a role in spatially organizing adaptors and membranous organelles. To test this hypothesis, we performed immunofluorescence localization of AP-3 and endosomal markers in SW13v− and v+ cells. In the absence of intermediate filaments, AP-3 was localized to the juxtanuclear region, and much of the punctate cytoplasmic staining seen in SW13v+ cells was absent (Figure 4, a and b). This modification in AP-3 subcellular distribution is due to adaptor redistribution and not to reduced AP-3 levels in SW13 v− cells, because the adaptor amount was identical in SW13 v− and v+ cells (Figure 3b). In accordance with differences in adaptor localization, two lysosomal membrane proteins, CD63 and LAMP I, which bind AP-3 in endosomes to then be delivered to lysosomes (Bonifacino and Traub, 2003; Peden *et al*., 2004), also were affected by the absence of intermediate filaments. In SW13v+ cells, CD63 and LAMP I punctate cytoplasmic staining was observed; however, in cells lacking vimentin, both proteins were concentrated in the juxtanuclear region (Figure 4, c–f). To confirm that this juxtanuclear pool was endocytically accessible, CD63 antibodies to an extracellular epitope were internalized from the cell surface. Internalized antibodies were concentrated around the nucleus in both cell types, yet in cells expressing vimentin, the punctate cytoplasmic labeling was more prominent (Figure S1a). This indicated that the juxtanuclear compartments labeled with late endosome-lysosome markers at steady state are accessible through the endocytic pathway. Early endosome distribution and function, assessed by transferrin receptor immunolocalization (Figure 4, g–h) or by endocytosis of Alexa-conjugated transferrin (Figure S1b) were indistinguishable between SW13v− and SW13v+ cells.

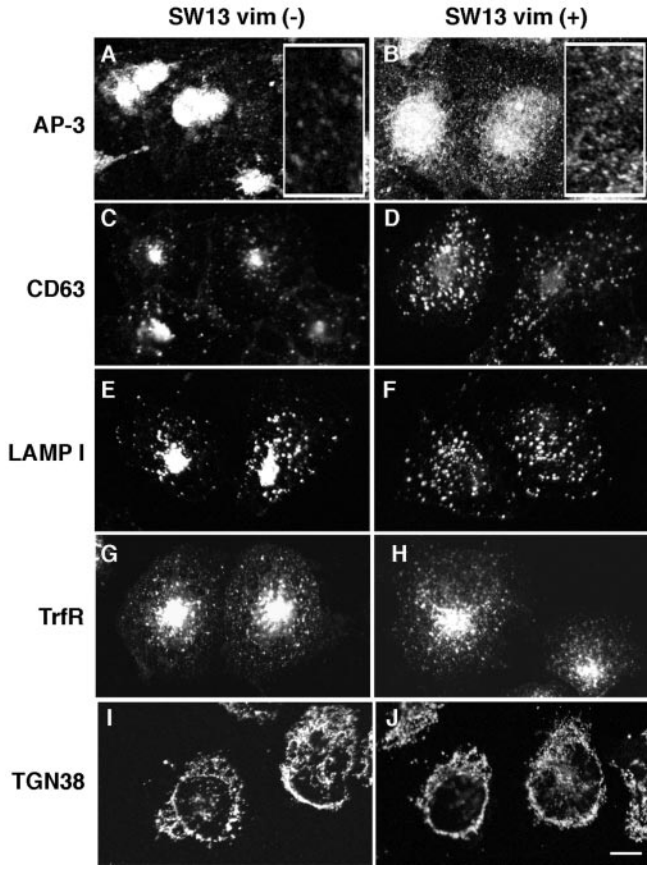

Figure 4. Lysosomal antigen distribution is modified in SW13 cells lacking intermediate filaments. SW13 v− and v+ cells were fixed and processed for immunofluorescence confocal microscopy. Cells were stained for AP-3 δ (a and b), CD63 (c and d), LAMP I (e and f), transferrin receptor (g and h), or TGN38 (I and j). AP-3 and lysosomal antigens are repositioned to the juxtanuclear region in cells lacking a vimentin cytoskeleton. In a and b, inserts depict an enlarged area of the cytoplasm. All experiments were done in duplicate coverslips on at least two independent experiments, and five to ten random fields were imaged per coverslip.

These results are in agreement with the observation that AP-3 does not bind the transferrin receptor cytosolic sorting signal (Dell'Angelica *et al*., 1999) and that this receptor is excluded from endosome domains coated with AP-3 (Peden *et al*., 2004). Moreover, they indicate that the initial stages of the endocytic pathway are not perturbed by the absence of intermediate filaments. To further assess whether the intermediate filament-deficient positioning phenotypes are restricted to late endosomal-lysosomal compartments; we analyzed the distribution of a *trans*-Golgi network marker, TGN38; a medial Golgi marker, GM130; and an endoplasmic reticulum marker, the KDEL receptor. We chose these markers because AP-3 is absent from their resident organelles (Peden *et al*., 2004). The distribution of TGN38 (Figure 4, i–j), GM130, and the KDEL receptor (our unpublished data) remained unaffected in cells lacking vimentin, further supporting the idea that the lack of intermediate filaments selectively affects organelles whose trafficking is regulated by AP-3.

The redistribution of AP-3 and the lysosomal membrane protein CD63 and LAMP I could reflect either a targeting defect to late endosomes/lysosomes and/or a redistribution of lysosomes to the juxtanuclear region. To explore these

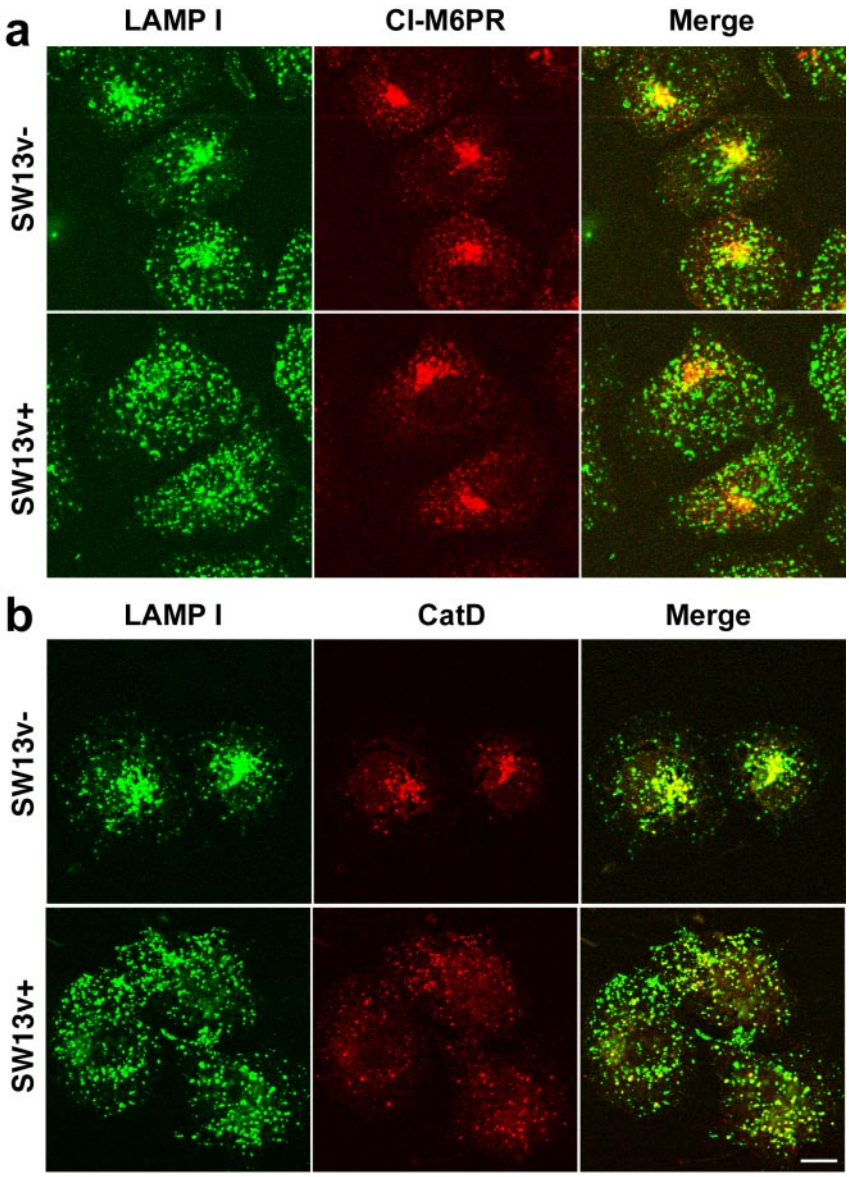

Figure 5. Cation-independent mannose-6-phosphate receptor distribution is not modified in SW13 cells lacking intermediate filaments. SW13 v− and v+ cells were fixed and processed for immunofluorescence confocal microscopy. Cells were costained with antibodies against the lysosomal antigens LAMP I and the cation-independent mannose-6-phosphate receptor (CI-M6PR) (a) or the lysosomal hydrolase cathepsin D (b). Lysosomal antigens are repositioned to the juxtanuclear region in cells lacking vimentin cytoskeleton, yet CI-M6PR distribution remains unaltered. Experiments were done in duplicate coverslips on at least two independent experiments.

options, we analyzed the distribution of the cation-independent mannose-6-phosphate receptor (CI-M6PR), a late endosome protein involved in the delivery of soluble proteins to the lysosome (Ghosh *et al*., 2003); and cathepsin D, a lysosomal hydrolase. Both molecules are trafficked to late stages of the endocytic pathway by AP-3–independent mechanisms (Ghosh *et al*., 2003). We hypothesized that if the vimentin-deficient phenotype is comprised in part by a lysosomal positioning defect, then the distribution of CI-M6PR should remain unaltered, whereas LAMP I and cathepsin D should relocalize to the juxtanuclear region (Figure 5). The subcellular distribution of the CI-M6PR was indistinguishable between SW13v+ and v− cells (Figure 5a), suggesting that the targeting of this receptor was not affected by the lack of intermediate filaments. In contrast, the luminal enzyme cathepsin D and the AP-3 cargo LAMP I were redistributed together to the juxtanuclear region in vimentin-deficient cells (Figure 5b). Thus, these results indicate that the absence of intermediate filaments affects the positioning of lysosome compartments without affecting the distribution of CI-M6PR.

We confirmed the AP-3 and lysosomal phenotypes in fibroblasts isolated from mice carrying an engineered vimentin deficiency (Figure 6) (Holwell *et al*., 1997; Gao and Sztul, 2001). Similar to SW13 cells, AP-3 (Figure 6, a and b) and the lysosomal antigens LAMP I and LAMP II (Figure 6, e and f) were redistributed to the juxtanuclear region in cells lacking vimentin (MTF16), although the phenotype was more subtle. However, in the absence of vimentin, a more dramatic phenotype was evident in these fibroblasts. LAMP I and II immunofluorescence levels and the size of the stained organelles were reduced compared with vimentin +/+ cells, thus suggesting that LAMP I and II sorting was affected by vimentin deficiency.

In summary, these results suggest a dual role for the intermediate filament cytoskeleton in providing 1) positional information for AP-3 and endo-lysosomal compartments and 2) regulating the sorting function of AP-3.

AP-3– and Vimentin-deficient Cells Share Late Endosomal-Lysosomal Phenotypes

We reasoned that if AP-3 and intermediate filaments play a role in the same compartment and/or sorting mechanism,

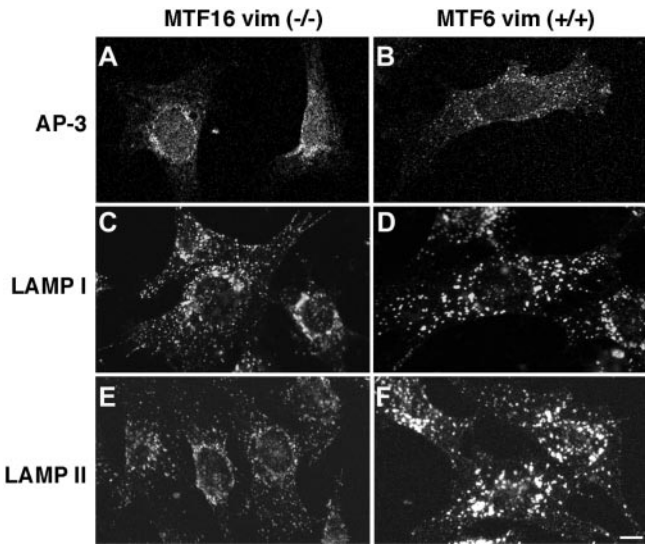

Figure 6. AP-3 and lysosomal antigen distribution are modified in fibroblasts from vimentin-deficient mice. MTF16 vimentin −/− and MTF6 vimentin +/+ cells were fixed and processed for immunofluorescence confocal microscopy. Cells were stained with antibodies to the AP-3 δ subunit (a and b), LAMP I (c and d), or LAMP II (e and f). As in SW13 cells, in fibroblasts lacking vimentin, AP-3 and lysosomal antigens are repositioned to the juxtanuclear region. Additionally, we observed differences in the size and intensity of LAMP-positive organelles. All experiments were done in duplicate coverslips on at least two independent experiments, and five to 10 random fields were imaged per coverslip.

then genetic deficiencies of these molecules may generate overlapping phenotypes. To test this hypothesis, we explored whether previously known, as well as new, AP-3–dependent phenotypes also could be observed in intermediate filament-deficient cells. We validated all of our experiments with vimentin-null fibroblasts in parallel assays performed in *mocha* fibroblasts deficient in the delta subunit of AP-3, a defect that leads to an AP-3-null phenotype (Kantheti *et al*., 1998).

AP-3 deficiency is known to modify the surface expression level of two lysosomal proteins LAMP I and LAMP II. These membrane proteins possess sorting motifs recognized by AP-3 (Le Borgne *et al*., 1998; Dell'Angelica *et al*., 1999, 2000). We confirmed these results in our *mocha* cells where the surface levels of LAMP I and LAMP II, determined by flow cytometry, were increased (Figure 7b). In addition, concomitant with the enlarged surface pool, total LAMP content was increased in AP-3–deficient cells (Figure 7a), a previously unreported phenotype. In fact, the percentage of total LAMP protein found on the cell surface actually decreases slightly in AP-3–deficient cells (Figure 7c). The total and surface level LAMP II phenotypes were confirmed by immunoblot and selective biotinylation of the cell surface (Figure 7d). To determine whether the changes in LAMP content were restricted to AP-3 cargoes, we used as a control a membrane protein whose sorting signal does not bind to AP-3, transferrin receptor (Dell'Angelica *et al*., 1999). Both transferrin receptor surface levels and total content were not increased in *mocha* cells, indicating that the changes in LAMP content were restricted to AP-3 cargoes (Figure 7d). We next determined whether the absence of intermediate filaments could similarly perturb LAMP levels without affecting transferrin receptor levels. Strikingly, although transferrin receptor levels were identical between vimentin-expressing and deficient cells, we observed a decrease in the total LAMP levels in vimentin-null MTF cells by flow cytometry (Figure 7a). The decreased total LAMP content was paralleled by a decreased surface expression of the lysosomal antigens (Figure 7b). However, the proportion of total LAMP protein found at the cell surface increased slightly in vimentin-deficient cells (Figure 7c). We confirmed these results by immunoblot analysis of the total and surface biotinylated LAMP II in wild-type and vimentin-deficient fibroblasts (Figure 7e). Vimentin-deficient cells possessed reduced total and surface LAMP II levels, yet transferrin receptor total and surface levels were not affected by the absence of filaments. These results are consistent with the hypothesis that AP-3 and intermediate filament deficiencies selectively regulate the trafficking of the lysosomal cargoes LAMP I and LAMP II, but not the targeting of other endosomal proteins like transferrin receptor.

Because LAMP content changes were divergent between AP-3 and vimentin-null cells, although still restricted to AP-3 cargoes, we decided to explore additional AP-3–dependent phenotypes. Neuronal and nonneuronal AP-3–deficient cells are characterized by a reduction in vesicular ionic zinc stores (Kantheti *et al*., 1998, 2003; Yang *et al*., 2000; Falcon-Perez *et al*., 2002; Martina *et al*., 2003). In fibroblasts, vesicular ionic zinc is present in late endosomal and lysosomal compartments, providing a tool to functionally assess these compartments (Kobayashi *et al*., 1999). We assessed vesicular zinc by flow cytometry using the zinc-specific fluoroprobe zinquin (Zalewski *et al*., 1994). The specificity of the signal was demonstrated either by omitting the zinc-loading or zinquin-labeling steps, both of which abolished the fluorescent signal (Salazar *et al*., 2004a). As reported previously, the absence of functional AP-3 in *mocha* cells severely diminished the vesicular zinc stores (Figure 8a). The zinquin fluorescence levels were 18 times lower in *mocha* fibroblasts than in cells expressing functional AP-3 (Figure 8c). Strikingly, similar to the *mocha* zinc transport phenotype, skin fibroblasts derived from engineered vimentin-deficient mice (MTF16), accumulated 40 times less zinquin dye than fibroblasts derived from a wild-type littermate (Figure 8, b and c). These results show that deficiencies in AP-3 and vimentin similarly affect the luminal ionic composition of endocytic organelles.

The luminal ionic composition of the endocytic pathway is controlled in part by the inward flow of chloride (Sonawane and Verkman, 2003; Faundez and Hartzell, 2004). In particular, an endosomal-lysosomal chloride channel, ClC-3, is trafficked by AP-3–dependent mechanisms both in neuronal and nonneuronal cells (Salazar *et al*., 2004a). Members of the ClC-3 chloride channel family are necessary for the acidification of endocytic compartments (Faundez and Hartzell, 2004), thus suggesting that AP-3 and vimentin deficiencies may impair the acidification of endocytic compartments. We explored this hypothesis using the pH-sensitive dye Lysosensor Green DND-189, which reports organelles in a pH range close to 5 (pK_a of 5.2) (Lin *et al*., 2001). Flow cytometry analysis revealed that AP-3–deficient *mocha* cells possessed a significantly decreased labeling with Lysosensor Green compared with cells rescued by the expression of the delta subunit (Figure 9, a and c). In vivo confocal microscopy confirmed that the reduction in staining was due to a fluorescence reduction in vesicular compartments (Figure 9d). Similar to *mocha* cells, labeling of vimentin-deficient fibroblasts with the pH-sensitive dye was less efficient (Figure 9, b–c), due mainly to a reduction in the amount of dye-labeled organelles (Figure 9d). Thus, our results indicate that acidic organelles are similarly affected in cells lacking either AP-3

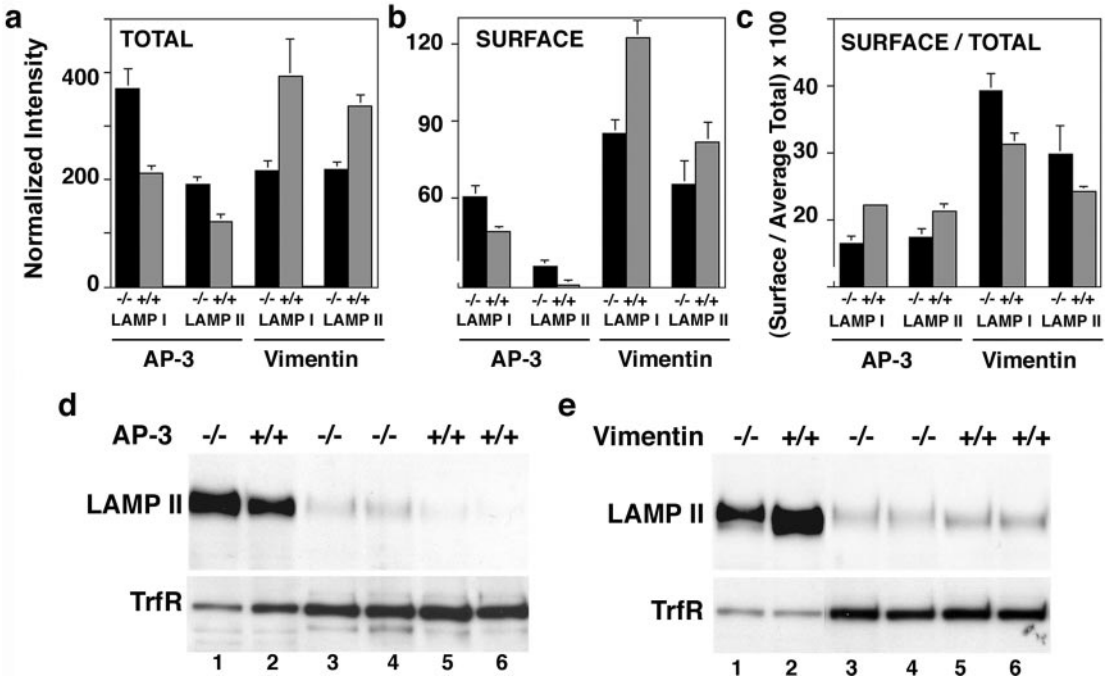

Figure 7. Total and surface levels of LAMP I and II are altered in AP-3 −/− and vimentin −/− fibroblasts. (a and b) Fixed cells were stained for LAMP I and II either in the presence or absence of saponin to assess total (a) or surface (b) staining, respectively. Mean fluorescence intensity was analyzed by flow cytometry, and staining was normalized by subtracting the mean fluorescence values of stainings lacking primary antibodies. Both total and surface staining of LAMPs were increased in AP-3 −/− cells compared with controls. In contrast, both total and surface staining of LAMP I and II was decreased in vimentin −/− cells (n = 3, triplicate asays). (c) Percentage of total LAMP I and II found at the surface was calculated from a and b. The percentage of LAMP at the surface is decreased in cells deficient for AP-3 and increased in cells deficient for vimentin compared with wild-type controls. (d and e) Fibroblasts were surface biotinylated, lysed and biotinylated proteins isolated with avidin beads. Precipitated proteins (lanes 3–6) or 5% of input (lanes 1 and 2) were blotted for either LAMP II or the transferrin receptor. Both total and surface levels of LAMP II are increased in AP-3 −/− fibroblasts (d). Total and surface levels of LAMP II are decreased in vimentin −/− fibroblasts (e). Surface levels of the transferrin receptor remain unchanged. Controls from nonbiotinylated lysates did not result in precipitation of either LAMP II or the transferrin receptor (our unpublished data). (d and e) Lanes 3 and 4 and 5 and 6 are duplicate assays of the biotinylation (n = 2, independent experiments).

or an intermediate filament cytoskeleton. This evidence further supports the notion that AP-3 and the vimentin cytoskeleton play a role in the mechanisms controlling the luminal ionic composition of endocytic organelles.

If phenotypes can be predicted in vimentin-null cells by analogy with AP-3 deficiency, then previously unsuspected AP-3 deficiency phenotypes should be predictable from vimentin-null cells. Intermediate filaments have been suggested to be involved in the formation of autophagic vacuoles, an organelle fated to fuse with lysosomes (Blankson *et al*., 1995; Kim and Klionsky, 2000). However, there has been no indication that AP-3 may participate in the formation of autophagic vacuoles, although LAMP II, an AP-3 cargo molecule, regulates autophagosome cellular content (Eskelinen *et al*., 2002). We focused on this organelle because a late endosome/lysosome intermediate can be detected using MDC, a florescent probe that partitions into the biochemical environment found in these vacuoles (Biederbick *et al*., 1995; Biederbick *et al*., 1999; Niemann *et al*., 2000; Munafo and Colombo, 2001). Flow cytometry analysis revealed that vimentin-null fibroblasts (MTF16) have a 42% reduction in monodansylcadaverine staining compared with wild-type fibroblasts (Figure 10, a and e). This change in fluorescence intensity also was observed in cells imaged in vivo by two-photon microscopy (Figure 10, c and e). The reduction in the monodansylcadaverine staining observed by flow cytometry in MTF16 cells was due to a reduction in the size and intensity of labeling of monodansylcadaverine-positive compartments. Notably, in the absence of functional AP-3, monodansylcadaverine staining was similarly reduced both by flow cytometry as well as microscopy (Figure 10, b and d). Similar to vimentin-null cells, the size and fluorescence intensity of the monodansylcadaverine-positive organelles was reduced in *mocha* cells (Figure 10, d and e). These phenotypes were rescued by reexpression of the delta AP-3 subunit into *mocha* cells, demonstrating their strict dependence on AP-3. Thus, our results indicate that novel AP-3-null phenotypes can be predicted from membrane-trafficking deficiencies found in intermediate filament-defective cells. Collectively, these results provide evidence that the roles of AP-3 and intermediates filament converge upon the same organelle and/or sorting mechanism.

DISCUSSION

The intermediate filament cytoskeleton has emerged as a key structural element in various cell types and tissues (Coulombe *et al*., 2000), yet its relationship with membrane protein sorting machineries has not been explored. Herein, we describe an association between intermediate filament proteins and the adaptor AP-3 through its β3 subunit. Several lines of evidence support our conclusion. First, AP-3 forms a sedimentable complex with intermediate filaments that can be immunoisolated free of tubulin and microtubule and actin-interacting proteins. This complex can be assembled in vitro between recombinant filament proteins and

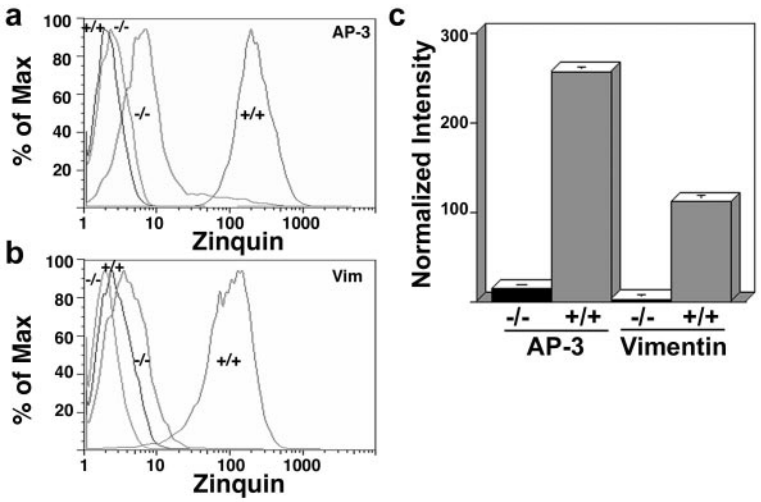

Figure 8. Vesicular zinc content is reduced in cells lacking either AP-3 or intermediate filaments. AP-3 −/−, AP-3 −/− cells rescued by transfection of the δ subunit, vimentin −/− and vimentin +/+ fibroblasts were stained with the zinc-specific dye zinquin. Mean fluorescence intensity was analyzed by flow cytometry and normalized by subtracting the mean fluorescence values of nonstained cells. (a and b) Unstained cells are shown by the far left traces. Both AP-3–deficient (a) and vimentin-deficient (b) fibroblasts possess decreased vesicular zinc content as reflected by the reduced zinquin fluorescence. (c) Quantification of a and b (n = 2, quintuplicate assays).

isolated AP-3 heterotetramers or β3 subunits. In addition, binding of AP-3 to intermediate filament networks also can be visualized in vivo, both morphologically and biochemically. Second, two different cell systems deficient for intermediate filaments reveal changes in the positioning of the adaptor AP-3 and membranous organelles whose function depends on AP-3. Third, consistent with a sorting defect, we demonstrated that vesicular zinc phenotypes characteristic of AP-3–deficient *mocha* fibroblasts (Kantheti *et al*., 1998, 2003; Yang *et al*., 2000; Falcon-Perez *et al*., 2002; Martina *et al*., 2003) as well as organellar pH defects seen in AP-3-null cells are both recapitulated in intermediate filament-deficient cells. Moreover, vimentin-null fibroblasts selectively affect the content of AP-3 cargoes LAMP I and LAMP II, without affecting the levels of other endosomal markers. Finally, based on the hypothesis that AP-3 and intermediate filaments converge on the same compartment/sorting mechanism, we have successfully predicted a previously unknown autophagic phenotype in AP-3-null *mocha* cells.

Although in all of our biochemical assays we provide evidence of specificity ex vivo, the strongest support for the adaptor AP-3–filament interaction derives from the common phenotypes found in genetically deficient cells, namely, defective zinquin, LysoSensor, and MDC staining, all of which reflect changes in the luminal composition of endocytic organelles. Defective zinc transport is likely the best defined phenotype found in neuronal and nonneuronal cells derived from pigment dilution/storage disease mouse models deficient in AP-3 subunits (Kantheti *et al*., 1998, 2003; Yang *et al*., 2000; Falcon-Perez *et al*., 2002; Martina *et al*., 2003). Strikingly, vimentin-null fibroblasts also possess a severely impaired zinc uptake similar to the phenotype found in AP-3–deficient cells. Zinc transport defects are not a generalized response to perturbations in the late endosome/lysosome pathway. Other pigment dilution/storage disease loci involved in the biogenesis of late endosome/lysosome compartments do not compromise zinc transport (Falcon-Perez *et al*., 2002; Martina *et al*., 2003), suggesting that AP-3 and intermediate filaments act in proximity in a similar organelle or mechanism.

Because luminal zinc content was altered, we predicted that other luminal characteristics also might be affected by both AP-3 and vimentin deficiencies. Late endocytic organelles whose traffic is regulated by AP-3 are characterized by their acidity. To determine whether cells lacking either AP-3 or vimentin possess a defect in the luminal ionic composition of endosomes, we used a pH-sensitive dye. We predicted a decreased content of acidic organelles based on our recent description of a chloride channel (ClC-3) whose trafficking to endosome-derived organelles is controlled by AP-3 (Salazar *et al*., 2004a). Members of this channel family play a role providing an anionic shunt that counterbalances the opposing electrical gradient created by the luminal buildup of protons (Faundez and Hartzell, 2004). This in turn favors further acidification of endosomal and lysosomal compartments (Sonawane and Verkman, 2003; Faundez and Hartzell, 2004). Consistently, we found a reduced labeling of organelles with Lysosensor Green in *mocha* cells. These compartments likely correspond to late endosomes and lysosomes, because the pH of these organelles is the closest to the pK_a of this dye (5.2) (Sonawane and Verkman, 2003; Faundez and Hartzell, 2004). Similarly, vimentin-deficient cells displayed a reduced labeling with Lysosensor Green, suggesting that the luminal pH of endocytic compartments also is impaired in vimentin-null cells. We also used another fluorescent probe to assess the luminal status of endocytic organelles, MDC. This dye acts as a solvent polarity probe and fluoresces in apolar-acidic environments (Niemann *et al*., 2000) like the one found in the multilamelar endosomal intermediaries of autophagosomes (Biederbick *et al*., 1995; Biederbick *et al*., 1999; Munafo and Colombo, 2001, 2002). Evidence from yeast and mammalian cells is consistent with the hypothesis that autophagosome dynamics and AP-3–dependent membrane traffic could be functionally linked. Autophagosome targeting to the yeast vacuole or the mammalian lysosome is dependent on membrane proteins, VAM3 and LAMP II, respectively, which are known to be recognized and targeted by AP-3 (Darsow *et al*., 1997; Darsow *et al*., 1998; Eskelinen *et al*., 2002). Our findings that vimentin-deficient cells possess a reduced number of organelles labeled by MDC support previous reports indicating that the content of autophagosomes is associated with the functional integrity of the intermediate filament cytoskeleton (Blankson *et al*., 1995). We have shown in vivo convergent phenotypes in AP-3– and vimentin-deficient cells by using dyes that report the luminal status of endocytic compartments. We hypothesize that these differences in the luminal ionic composition reflect AP-3– and vimentin-dependent changes in the content of membrane proteins controlling the luminal properties of endocytic organelles.

Cytokeratin-deficient mouse models and epithelial cell lines provide a precedent to the hypothesis that the inter-

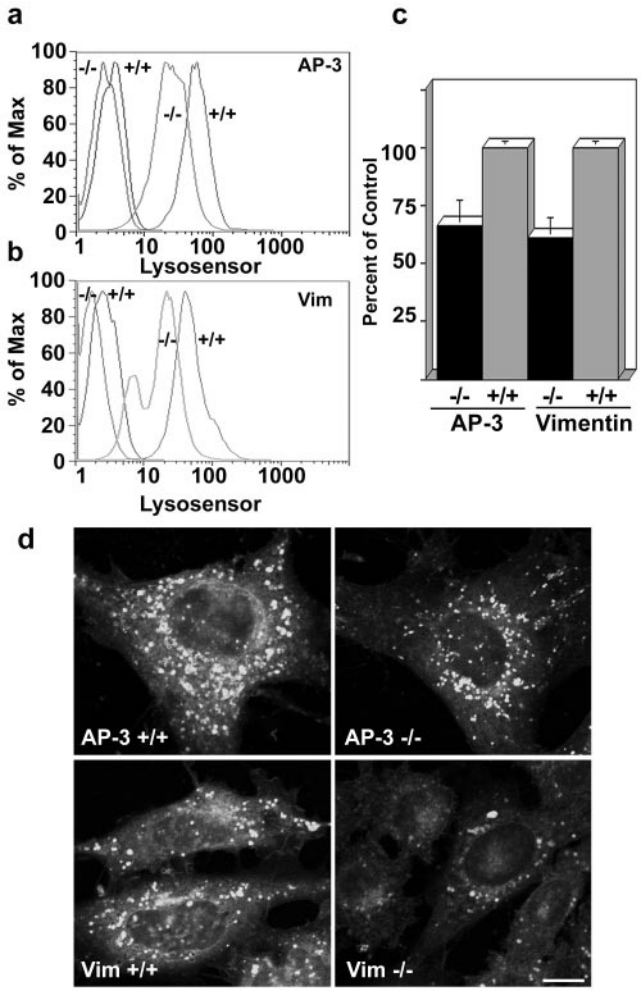

Figure 9. Lysosensor Green-positive organelles are decreased in both AP-3 −/− and vimentin −/− fibroblasts. (a and b) Fibroblasts were stained with Lysosensor Green DND-189 and fluorescence was analyzed by flow cytometry. Unstained cells are depicted by the far-left traces. Both AP-3–deficient (a) and vimentin-deficient (b) fibroblasts exhibit less Lysosensor staining compared with +/+ controls. (c) Quantification of a and b (n = 4, triplicate assays). Background fluorescence from unstained cells was subtracted from the mean fluorescence of stained cells to obtain a normalized mean. Data are depicted as percentage of control +/+ cells. (d) Fibroblasts stained with Lysosensor were imaged by confocal microscopy. Both vimentin −/− and AP-3 −/− cells had reduced number of Lysosensor-positive organelles.

mediate filament cytoskeleton regulates membrane protein composition via sorting mechanisms. Membrane proteins normally sorted to the apical pole are mistargeted to the basolateral domain in the absence of defined cytokeratins (Salas *et al*., 1997; Ameen *et al*., 2001; Toivola *et al*., 2004). We assessed defective sorting of AP-3–trafficked proteins by examining total and surface expression of known AP-3–trafficked molecules LAMP I and LAMP II. Our work and others demonstrates that in the absence of AP-3, surface levels of LAMP are increased (Le Borgne *et al*., 1998; Dell'Angelica *et al*., 1999, 2000). In addition to the surface level expression of LAMP, we also found that the total levels of these proteins are increased in *mocha* cells. Importantly, a central criterion to establish the selectivity of these LAMP phenotypes in AP-3–deficient cells is the observation that neither the total nor the surface levels of transferrin receptor are increased in the *mocha* background. Although the changes in the LAMP total and surface levels observed in vimentin-null cells are in the opposite direction of those observed in *mocha* cells, they remain restricted to AP-3 cargoes. Vimentin-null cells retain unperturbed transferrin receptor content despite the dramatic differences in LAMPs. The divergence in the cellular levels of LAMP found in AP-3 −/− and vimentin −/− cells could result from intermediate filaments playing additional roles in controlling the trafficking of lysosome-bound membrane proteins or in modulating the binding of factors to the ear of the β3 subunit. We have excluded a role of intermediate filaments in controlling LAMP biosynthesis. Pulse-chase experiments indicate that there are no appreciable differences in the synthesis of LAMP I and II among wild-type, *mocha*-, and vimentin-deficient cells (our unpublished data). However, the fact that transferrin receptor remains unaffected in AP-3- as well as in vimentin-null cells argues in favor of a role of filaments in the traffic of AP-3 cargoes.

Do other cytoskeletal components regulate late endosome/lysosome traffic? Multiple lines of evidence point to the involvement of the actin and microtubule cytoskeletons and their associated motors in membrane traffic through and to late endosome/lysosome compartments (Apodaca, 2001). Although we found no interaction of AP-3 with components of the microtubule and actin cytoskeleton, our results do not exclude the participation of the microtubule or actin cytoskeletons. Quite the contrary, intermediate filaments, microtubules, and microfilaments are intertwined networks bridged by motor and nonmotor molecules (Prahlad *et al*., 1998; Helfand *et al*., 2002; Leung *et al*., 2002; Helfand *et al*., 2003, 2004). Thus, it is possible that these three cytoskeletal systems may regulate in a coordinated manner the position and function of late endosomes/lysosomes. Genetic deficiencies support these relationships. Charcot-Marie-Tooth disease, a neuropathy that compromises axons (type II), can be triggered by genetic defects either in kinesin 1B (Zhao *et al*., 2001), intermediate filament subunits (Tanaka and Hirokawa, 2002), or the late endosome/lysosome GTPase rab7 (Verhoeven *et al*., 2003). In addition, Hermansky-Pudlak disease comprises a series of genetic deficiencies in mechanisms controlling the biogenesis of lysosomes. Human Hermansky-Pudlak and mouse pigment dilution/storage pool disease loci gene products have been shown to interact with various cytoskeletal components. For example, the mouse *pearl*, *sandy*, and *pallid* alleles affect the β3A subunit of AP-3, dysbindin, and pallidin, respectively. These three molecules each interact with components of the cytoskeleton (Falcon-Perez *et al*., 2002; Clark *et al*., 2003; Li *et al*., 2003). Interactions between components of the cytoskeleton and gene products involved in the biogenesis of lysosomes suggest that, in addition to controlling the traffic of membrane protein cargoes, these molecular interactions also could control the position of endo-lysosomal compartments in the cytoplasm by modulating cytoskeletal elements. Our data indicate that intermediate filament deficiencies change the steady-state cellular distribution of lysosomal compartments. This positioning phenotype also has been described in pigment dilution/storage disease alleles *pale ear* and *light ear*, although not in AP-3–deficient models (Nazarian *et al*., 2003). However, *pale ear and light ear* do not appreciably affect sorting of lysosomal resident proteins (Dell'Angelica *et al*., 2000). Our observations suggest that intermediate filament deficiency phenotypes bridge the sorting defects seen in pigment dilution/storage pool disease AP-3 alleles *mocha* and *pearl* and the positioning phenotypes observed in *pale ear* and *light ear*.

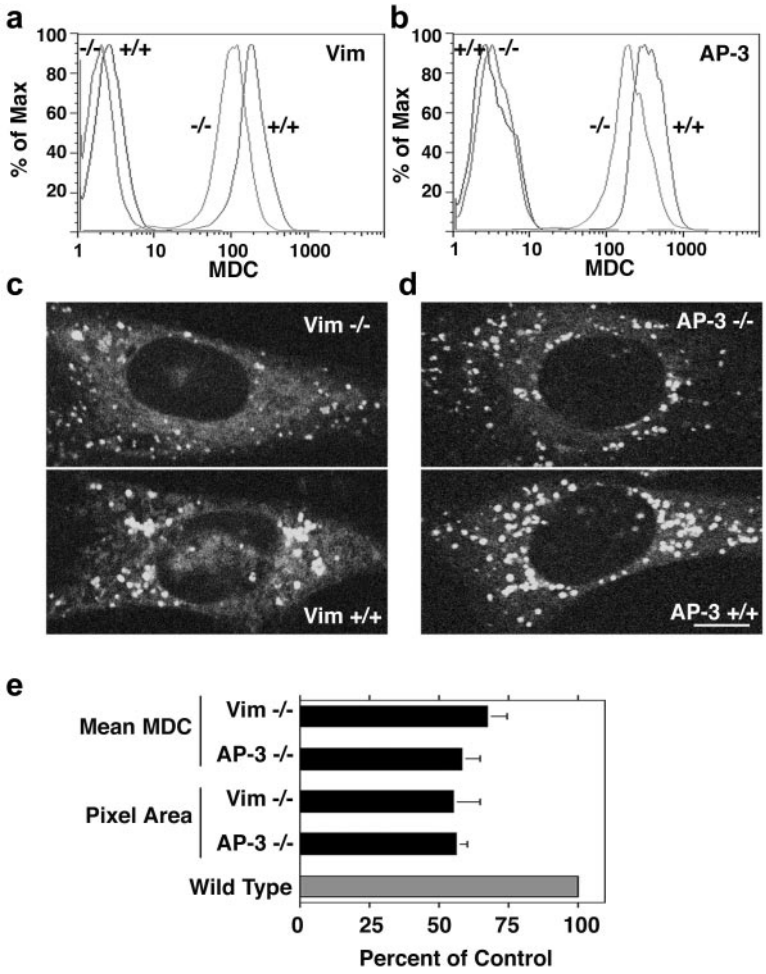

Figure 10. Staining of monodansyl cadaverine-positive organelles is decreased in both AP-3 −/− and vimentin −/− fibroblasts. (a and b) Fibroblasts were stained with MDC, and fluorescence was analyzed by flow cytometry. Unstained cells are depicted by the far-left traces. Both vimentin-deficient (a) and AP-3–deficient (b) fibroblasts exhibit less MDC staining compared with +/+ controls. (c and d) Fibroblasts stained with MDC were imaged by two-photon microscopy. Both vimentin −/− (c) and AP-3 −/− (d) cells had smaller and less intense staining of MDC-positive vacuoles. (e) Quantification of a–d (n = 3, triplicate assays). MDC mean fluorescence intensity was assessed by flow cytometry. Background fluorescence from unstained cells was subtracted from the mean fluorescence of stained cells to obtain a normalized mean. Pixel area of MDC vacuoles from images of MDC-stained fibroblasts was assessed using MetaMorph software. In both cases, +/+ fibroblasts were set to 100%. A ~45% decrease was seen in both total intensity per cell and autophagic vacuole size in both vimentin −/− and AP-3 −/− fibroblasts.

In summary, we have documented a previously unsuspected association between intermediate filaments and the membrane protein sorting machinery. Our results suggest a novel role for intermediate filaments in dictating the subcellular localization and adaptor AP-3–dependent traffic in endocytic organelles. These observations suggest that the cytoskeletal asymmetry observed in polarized cells is coordinated with the machinery controlling the asymmetric protein composition of membrane domains.

ACKNOWLEDGMENTS

This work was supported by grants from CND-Merck Scholar Award, Melanoma Research Foundation, and National Institutes of Health grants R01 NS42599-01A1 and 5P30AR042687-090044.

REFERENCES

Ameen, N.A., Figueroa, Y., and Salas, P.J. (2001). Anomalous apical plasma membrane phenotype in CK8-deficient mice indicates a novel role for intermediate filaments in the polarization of simple epithelia. J. Cell Sci. *114*, 563–575.

Apodaca, G. (2001). Endocytic traffic in polarized epithelial cells: role of the actin and microtubule cytoskeleton. Traffic *2*, 149–159.

Biederbick, A., Kern, H.F., and Elsasser, H.P. (1995). Monodansylcadaverine (MDC) is a specific in vivo marker for autophagic vacuoles. Eur J. Cell Biol. *66*, 3–14.

Biederbick, A., Rose, S., and Elsasser, H.P. (1999). A human intracellular apyrase-like protein, LALP70, localizes to lysosomal/autophagic vacuoles. J. Cell Sci. *112*, 2473–2484.

Blankson, H., Holen, I., and Seglen, P.O. (1995). Disruption of the cytokeratin cytoskeleton and inhibition of hepatocytic autophagy by okadaic acid. Exp. Cell Res. *218*, 522–530.

Bonifacino, J.S., and Traub, L.M. (2003). Signals for sorting of transmembrane-proteins to endosomes and lysosomes. Annu. Rev. Biochem. *72*, 395–447.

Clark, R.H., Stinchcombe, J.C., Day, A., Blott, E., Booth, S., Bossi, G., Hamblin, T., Davies, E.G., and Griffiths, G.M. (2003). Adaptor protein 3-dependent microtubule-mediated movement of lytic granules to the immunological synapse. Nat. Immunol. *4*, 1111–1120.

Clift-O'Grady, L., Desnos, C., Lichtenstein, Y., Faundez, V., Horng, J.T., and Kelly, R.B. (1998). Reconstitution of synaptic vesicle biogenesis from PC12 cell membranes. Methods *16*, 150–159.

Coulombe, P.A., Bousquet, O., Ma, L., Yamada, S., and Wirtz, D. (2000). The 'ins' and 'outs' of intermediate filament organization. Trends Cell Biol. *10*, 420–428.

Darsow, T., Burd, C.G., and Emr, S.D. (1998). Acidic di-leucine motif essential for AP-3-dependent sorting and restriction of the functional specificity of the Vam3p vacuolar t-SNARE. J. Cell Biol. *142*, 913–922.

Darsow, T., Rieder, S.E., and Emr, S.D. (1997). A multispecificity syntaxin homologue, Vam3p, essential for autophagic and biosynthetic protein transport to the vacuole. J. Cell Biol. *138*, 517–529.

Dell'Angelica, E.C., Aguilar, R.C., Wolins, N., Hazelwood, S., Gahl, W.A., and Bonifacino, J.S. (2000). Molecular characterization of the protein encoded by the Hermansky-Pudlak syndrome type 1 gene. J. Biol. Chem. *275*, 1300–1306.

Dell'Angelica, E.C., Klumperman, J., Stoorvogel, W., and Bonifacino, J.S. (1998). Association of the AP-3 adaptor complex with clathrin. Science *280*, 431–434.

Dell'Angelica, E.C., Ohno, H., Ooi, C.E., Rabinovich, E., Roche, K.W., and Bonifacino, J.S. (1997). AP-3, an adaptor-like protein complex with ubiquitous expression. EMBO J. *16*, 917–928.

Dell'Angelica, E.C., Shotelersuk, V., Aguilar, R.C., Gahl, W.A., and Bonifacino, J.S. (1999). Altered trafficking of lysosomal proteins in Hermansky-Pudlak syndrome due to mutations in the beta 3A subunit of the AP-3 adaptor. Mol. Cell *3*, 11–21.

Djabali, K., Zissopoulou, A., de Hoop, M.J., Georgatos, S.D., and Dotti, C.G. (1993). Peripherin expression in hippocampal neurons induced by muscle soluble factor(s). J. Cell Biol. *123*, 1197–1206.

Eskelinen, E.L., Illert, A.L., Tanaka, Y., Schwarzmann, G., Blanz, J., Von Figura, K., and Saftig, P. (2002). Role of LAMP-2 in lysosome biogenesis and autophagy. Mol. Biol. Cell *13*, 3355–3368.

Falcon-Perez, J.M., Starcevic, M., Gautam, R., and Dell'Angelica, E.C. (2002). BLOC-1, a novel complex containing the pallidin and muted proteins involved in the biogenesis of melanosomes and platelet-dense granules. J. Biol. Chem. *277*, 28191–28199.

Faundez, V., and Hartzell, H.C. (2004). Intracellular chloride channels: determinants of function in the endosomal pathway. Sci. STKE *2004*, RE8.

Faundez, V., Horng, J.T., and Kelly, R.B. (1997). ADP ribosylation factor 1 is required for synaptic vesicle budding in PC12 cells. J. Cell Biol. *138*, 505–515.

Faundez, V., Horng, J.T., and Kelly, R.B. (1998). A function for the AP3 coat complex in synaptic vesicle formation from endosomes. Cell *93*, 423–432.

Faundez, V., and Kelly, R.B. (2000). The AP-3 complex required for endosomal synaptic vesicle biogenesis is associated with a casein kinase ialpha-like isoform. Mol. Biol. Cell *11*, 2591–2604.

Feng, L., *et al*. (1999). The beta3A subunit gene (Ap3b1) of the AP-3 adaptor complex is altered in the mouse hypopigmentation mutant pearl, a model for Hermansky-Pudlak syndrome and night blindness. Hum. Mol. Genet. *8*, 323–330.

Gaidarov, I., Santini, F., Warren, R.A., and Keen, J.H. (1999). Spatial control of coated-pit dynamics in living cells. Nat. Cell Biol. *1*, 1–7.

Gao, Y., and Sztul, E. (2001). A novel interaction of the Golgi complex with the vimentin intermediate filament cytoskeleton. J. Cell Biol. *152*, 877–894.

Ghosh, P., Dahms, N.M., and Kornfeld, S. (2003). Mannose 6-phosphate receptors: new twists in the tale. Nat. Rev. Mol. Cell. Biol. *4*, 202–212.

Gillard, B.K., Clement, R., Colucci-Guyon, E., Babinet, C., Schwarzmann, G., Taki, T., Kasama, T., and Marcus, D.M. (1998). Decreased synthesis of glycosphingolipids in cells lacking vimentin intermediate filaments. Exp. Cell Res. *242*, 561–572.

Gillard, B.K., Thurmon, L.T., Harrell, R.G., Capetanaki, Y., Saito, M., Yu, R.K., and Marcus, D.M. (1994). Biosynthesis of glycosphingolipids is reduced in the absence of a vimentin intermediate filament network. J. Cell Sci. *107*, 3545–3555.

Gottlieb, T.A., Ivanov, I.E., Adesnik, M., and Sabatini, D.D. (1993). Actin microfilaments play a critical role in endocytosis at the apical but not the basolateral surface of polarized epithelial cells. J. Cell Biol. *120*, 695–710.

Hedberg, K.K., and Chen, L.B. (1986). Absence of intermediate filaments in a human adrenal cortex carcinoma-derived cell line. Exp. Cell Res. *163*, 509–517.

Helfand, B.T., Chang, L., and Goldman, R.D. (2003). The dynamic and motile properties of intermediate filaments. Annu. Rev. Cell Dev. Biol. *19*, 445–467.

Helfand, B.T., Chang, L., and Goldman, R.D. (2004). Intermediate filaments are dynamic and motile elements of cellular architecture. J. Cell Sci. *117*, 133–141.

Helfand, B.T., Mikami, A., Vallee, R.B., and Goldman, R.D. (2002). A requirement for cytoplasmic dynein and dynactin in intermediate filament network assembly and organization. J. Cell Biol. *157*, 795–806.

Holwell, T.A., Schweitzer, S.C., and Evans, R.M. (1997). Tetracycline regulated expression of vimentin in fibroblasts derived from vimentin null mice. J. Cell Sci. *110*, 1947–1956.

Holwell, T.A., Schweitzer, S.C., Reyland, M.E., and Evans, R.M. (1999). Vimentin-dependent utilization of LDL-cholesterol in human adrenal tumor cells is not associated with the level of expression of apoE, sterol carrier protein-2, or caveolin. J. Lipid Res. *40*, 1440–1452.

Huizing, M., Boissy, R.E., and Gahl, W.A. (2002). Hermansky-Pudlak syndrome: vesicle formation from yeast to man. Pigment Cell Res. *15*, 405–419.

Kantheti, P., Diaz, M.E., Peden, A.E., Seong, E.E., Dolan, D.F., Robinson, M.S., Noebels, J.L., and Burmeister, M.L. (2003). Genetic and phenotypic analysis of the mouse mutant mh2J, an Ap3d allele caused by IAP element insertion. Mamm. Genome *14*, 157–167.

Kantheti, P., *et al*. (1998). Mutation in AP-3 delta in the mocha mouse links endosomal transport to storage deficiency in platelets, melanosomes, and synaptic vesicles. Neuron *21*, 111–122.

Kim, J., and Klionsky, D.J. (2000). Autophagy, cytoplasm-to-vacuole targeting pathway, and pexophagy in yeast and mammalian cells. Annu. Rev. Biochem. *69*, 303–342.

Kobayashi, T., Beuchat, M.H., Lindsay, M., Frias, S., Palmiter, R.D., Sakuraba, H., Parton, R.G., and Gruenberg, J. (1999). Late endosomal membranes rich in lysobisphosphatidic acid regulate cholesterol transport. Nat. Cell Biol. *1*, 113–118.

Landon, F., Wolff, A., and de Nechaud, B. (2000). Mouse peripherin isoforms. Biol. Cell *92*, 397–407.

Le Borgne, R., Alconada, A., Bauer, U., and Hoflack, B. (1998). The mammalian AP-3 adaptor-like complex mediates the intracellular transport of lysosomal membrane glycoproteins. J. Biol. Chem. *273*, 29451–29461.

Leung, C.L., Green, K.J., and Liem, R.K. (2002). Plakins: a family of versatile cytolinker proteins. Trends Cell Biol. *12*, 37–45.

Li, W., *et al*. (2003). Hermansky-Pudlak syndrome type 7 (HPS-7) results from mutant dysbindin, a member of the biogenesis of lysosome-related organelles complex 1 (BLOC-1). Nat. Genet. *35*, 84–89.

Lin, H.J., Herman, P., Kang, J.S., and Lakowicz, J.R. (2001). Fluorescence lifetime characterization of novel low-pH probes. Anal. Biochem. *294*, 118–125.

Martina, J.A., Moriyama, K., and Bonifacino, J.S. (2003). BLOC-3, a protein complex containing the Hermansky-Pudlak syndrome gene products HPS1 and HPS4. J. Biol. Chem. *278*, 29376–29384.

Munafo, D.B., and Colombo, M.I. (2001). A novel assay to study autophagy: regulation of autophagosome vacuole size by amino acid deprivation. J. Cell Sci. *114*, 3619–3629.

Munafo, D.B., and Colombo, M.I. (2002). Induction of autophagy causes dramatic changes in the subcellular distribution of GFP-Rab24. Traffic *3*, 472–482.

Nakagawa, T., Setou, M., Seog, D., Ogasawara, K., Dohmae, N., Takio, K., and Hirokawa, N. (2000). A novel motor, KIF13A, transports mannose-6-phosphate receptor to plasma membrane through direct interaction with AP-1 complex. Cell *103*, 569–581.

Nazarian, R., Falcon-Perez, J.M., and Dell'Angelica, E.C. (2003). Biogenesis of lysosome-related organelles complex 3 (BLOC-3): a complex containing the Hermansky-Pudlak syndrome (HPS) proteins HPS1 and HPS4. Proc. Natl. Acad. Sci. USA *100*, 8770–8775.

Niemann, A., Takatsuki, A., and Elsasser, H.P. (2000). The lysosomotropic agent monodansylcadaverine also acts as a solvent polarity probe. J. Histochem. Cytochem. *48*, 251–258.

Peden, A.A., Oorschot, V., Hesser, B.A., Austin, C.D., Scheller, R.H., and Klumperman, J. (2004). Localization of the AP-3 adaptor complex defines a novel endosomal exit site for lysosomal membrane proteins. J. Cell Biol. *164*, 1065–1076.

Prahlad, V., Yoon, M., Moir, R.D., Vale, R.D., and Goldman, R.D. (1998). Rapid movements of vimentin on microtubule tracks: kinesin-dependent assembly of intermediate filament networks. J. Cell Biol. *143*, 159–170.

Qualmann, B., and Kessels, M.M. (2002). Endocytosis and the cytoskeleton. Int. Rev. Cytol. *220*, 93–144.

Robinson, M.S. (2004). Adaptable adaptors for coated vesicles. Trends Cell Biol. *14*, 167–174.

Salas, P.J., Rodriguez, M.L., Viciana, A.L., Vega-Salas, D.E., and Hauri, H.P. (1997). The apical submembrane cytoskeleton participates in the organization of the apical pole in epithelial cells. J. Cell Biol. *137*, 359–375.

Salazar, G., and Gonzalez, A. (2002). Novel mechanism for regulation of epidermal growth factor receptor endocytosis revealed by protein kinase A inhibition. Mol. Biol. Cell *13*, 1677–1693.

Salazar, G., Love, R., Styers, M.L., Werner, E., Peden, A., Rodriguez, S., Gearing, M., Wainer, B.H., and Faundez, V. (2004a). AP-3-dependent mechanisms control the targeting of a chloride channel (ClC-3) in neuronal and non-neuronal cells. J. Biol. Chem. *279*, 25430–25439.

Salazar, G., Love, R., Werner, E., Doucette, M.M., Cheng, S., Levey, A., and Faundez, V. (2004b). The zinc transporter ZnT3 interacts with AP-3 and it is

preferentially targeted to a distinct synaptic vesicle subpopulation. Mol. Biol. Cell *15*, 575–587.

Salem, N., Faundez, V., Horng, J.T., and Kelly, R.B. (1998). A v-SNARE participates in synaptic vesicle formation mediated by the AP3 adaptor complex. Nat. Neurosci. *1*, 551–556.

Sarria, A.J., Panini, S.R., and Evans, R.M. (1992). A functional role for vimentin intermediate filaments in the metabolism of lipoprotein-derived cholesterol in human SW-13 cells. J. Biol. Chem. *267*, 19455–19463.

Sonawane, N.D., and Verkman, A.S. (2003). Determinants of [Cl^-] in recycling and late endosomes and Golgi complex measured using fluorescent ligands. J. Cell Biol. *160*, 1129–1138.

Tanaka, Y., and Hirokawa, N. (2002). Mouse models of Charcot-Marie-Tooth disease. Trends Genet. *18*, S39–44.

Toivola, D.M., Krishnan, S., Binder, H.J., Singh, S.K., and Omary, M.B. (2004). Keratins modulate colonocyte electrolyte transport via protein mistargeting. J. Cell Biol. *164*, 911–921.

Verhoeven, K., *et al*. (2003). Mutations in the small GTP-ase late endosomal protein RAB7 cause Charcot-Marie-Tooth type 2B neuropathy. Am. J. Hum. Genet. *72*, 722–727.

Yang, W., Li, C., Ward, D.M., Kaplan, J., and Mansour, S.L. (2000). Defective organellar membrane protein trafficking in Ap3b1-deficient cells. J. Cell Sci. *113*, 4077–4086.

Zalewski, P.D., Millard, S.H., Forbes, I.J., Kapaniris, O., Slavotinek, A., Betts, W.H., Ward, A.D., Lincoln, S.F., and Mahadevan, I. (1994). Video image analysis of labile zinc in viable pancreatic islet cells using a specific fluorescent probe for zinc. J. Histochem. Cytochem. *42*, 877–884.

Zhao, C., *et al*. (2001). Charcot-Marie-Tooth disease type 2A caused by mutation in a microtubule motor KIF1Bbeta. Cell *105*, 587–597.